

# Local Structures of Mechanically Alloyed $\text{Al}_{70}\text{Cu}_{20}\text{Fe}_{10}$ Nanocomposites Studied by XRD and XAFS

Shilong Yin<sup>1\*</sup>, Liying Qian<sup>1</sup>, Bo He<sup>2</sup>, Shaobo Zou,<sup>2</sup> Qing Bian<sup>3</sup>,  
and Shiqiang Wei<sup>2</sup>

<sup>1</sup> Institute of Science, Hohai University, Nanjing 210098; <sup>2</sup> National Synchrotron Radiation Laboratory, University of Science and Technology of China, Hefei, 230029; <sup>3</sup> Institute of Science, PLAUST, Nanjing 210007, P.R. China

**Abstract.** Ternary  $\text{Al}_{70}\text{Cu}_{20}\text{Fe}_{10}$  alloy nano-composites prepared by mechanical alloying are characterized by X-ray diffraction (XRD) and X-ray absorption fine structure (XAFS). The results indicate that after milled for 10 hours, the coordination environment around Cu atoms is changed largely and becomes disordered, but the local structure of Fe atoms still remains as that of  $\alpha$ -Fe. This indicates the forming of inter-metallic compound  $\text{Al}_2\text{Cu}$  with body center cubic structure. Even if the milling time is extended to 40 hours, only small amount of  $\alpha$ -Fe can be alloyed to produce Al-Fe-Cu alloy. However, the annealing treatment at 700 °C can drive the  $\alpha$ -Fe to incorporate into the  $\text{Al}_2\text{Cu}$  compound to form an icosahedral alloy phase.

**Keywords:**  $\text{Al}_{70}\text{Cu}_{20}\text{Fe}_{10}$ , Annealing, XRD, EXAFS.

**PACS:** 81.40.Ef, 61.10.Nz, 61.10.Ht.

## INTRODUCTION

Recently, the study of stable quasi-crystal (QC) alloys in low dimensional form is a subject of growing interest due to their excellent performance in catalytic activity, hydrogen storage and mitigating the risk of the brittle nature [1]. The formation of icosahedral QC phase in a mechanical alloying (MA) AlCuFe powder mixture has been studied using various methods such as XRD, energy-dispersive X-ray microanalysis, TEM and X-ray photoelectron spectroscopy, where  $\text{Al}_{70}\text{Cu}_{20}\text{Fe}_{10}$  is the most extensively studied [2-5]. It shows that the milling time and annealing treatment are two crucial factors to the final phase evolution of the MA AlCuFe system [2,4]. Since in quasicrystals there are many different strictly quasiperiodic atomic arrangements, some structural characterization technique capable of distinguishing the chemical species is of particular importance [6].

In this work, XRD and XAFS techniques are used to study the effects of the MA process and thermal treatments on the formation of quasicrystals in  $\text{Al}_{70}\text{Cu}_{20}\text{Fe}_{10}$ . XRD results reveal from the aspect of average lattice the phase development in the milling and annealing process. A further understanding of the phase composition, especially of the QC phase, is obtained by XAFS study. The distinct features of Fe and Cu edge XAFS spectra in the MA process allow

us to clarify the different role of Fe and Cu atoms in the phase development from a local structural viewpoint. This work can also shed light on the occupation of the different chemical species in the quasicrystals.

## EXPERIMENTAL

Elemental powders of Al, Fe and Cu (200 mesh, 99.9% purity) corresponding to the nominal composition  $\text{A}_{70}\text{Cu}_{20}\text{Fe}_{10}$  were milled in a cylindrical stainless-steel vial of a planetary ball mill for 5, 10, 20 and 40 h at room temperature. The weight of the mixed powders was about 15 g each time and the ball-to-powder weight ratio was 30:1. To minimize oxygen contamination, the milling treatments were performed under argon atmosphere. We added ethanol as a lubricant agent to prevent excessive welding of the powders to the balls and container walls during the process. The milled powders have been annealed at 700 °C for 4 hours under a vacuum of  $1\times 10^{-3}$  Pa.

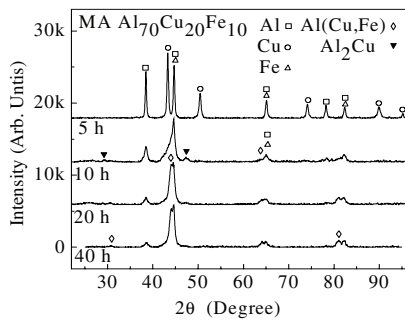
The crystal structures of the as-milled and heat-treated samples were characterized with a D/max-rA rotating target diffractometer using Cu-K $\alpha$  radiation, operated at 60 kV and 150 mA. The Fe and Cu K-edge XAFS measurements for all samples were performed at the beamline U7C of National Synchrotron Radiation Laboratory of China (NSRL) with a storage ring of 0.8 GeV and a maximum current of 300 mA. The fixed-

exit Si(111) flat double crystals were used as monochromator. XAFS data were analyzed by the NSRLXAFS software package [7].

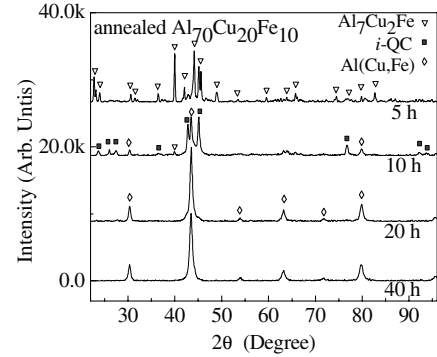
## RESULTS

Figure 1 shows the XRD patterns for the as-milled MA  $\text{Al}_{70}\text{Cu}_{20}\text{Fe}_{10}$  powders with milling time. It can be observed that the diffraction peaks corresponding to the fcc Cu phase disappear yet the Al phase remains while the milling time is up to 10 h. Several new peaks at  $29.2^\circ$ ,  $42.6^\circ$  and  $47.3^\circ$  can be observed. This indicates that a new phase of  $\text{Al}_2\text{Cu}$  compound is formed.<sup>8</sup> Increasing the milling time to 20 and 40 h, besides diffraction peaks of Al and  $\text{Al}_2\text{Cu}$  phases, weak diffraction peaks corresponding to the  $\text{AlCu}$  and  $\text{Al}(\text{Cu}, \text{Fe})$  solid solutions can be found.

The XRD patterns of different MA  $\text{Al}_{70}\text{Cu}_{20}\text{Fe}_{10}$  alloy samples annealed at  $700^\circ\text{C}$  for 4 h are shown in Figure 2. The XRD results indicate that the bcc structural  $\alpha$ -Fe can react with the  $\text{AlCu}$  alloy and the fcc structural Al to form an  $\text{AlCuFe}$  alloy. For the annealed  $\text{Al}_{70}\text{Cu}_{20}\text{Fe}_{10}$  (5h), the resultant product was almost composed of a single phase of  $\text{Al}_7\text{Cu}_2\text{Fe}$  compound [8]. Remarkably, the XRD pattern of the annealed  $\text{Al}_{70}\text{Cu}_{20}\text{Fe}_{10}$  (10h) shows that an icosahedral QC phase is formed mainly, along with small fraction of  $\text{Al}(\text{Cu}, \text{Fe})$  solid solution and  $\text{Al}_7\text{Cu}_2\text{Fe}$  compound. The strong diffraction peaks of superlattice at about  $23.7^\circ$ ,  $26.0^\circ$ ,  $27.4^\circ$ ,  $42.8^\circ$  and  $45.1^\circ$  are the characteristic of the icosahedral QC phase with F-type structure, which are similar to those observed by Barua et al [2]. It is also surprising that the as-annealed  $\text{Al}_{70}\text{Cu}_{20}\text{Fe}_{10}$  (20 and 40 h) show essentially a single phase of  $\text{Al}(\text{Cu}, \text{Fe})$  solid solution, suggesting that the  $\text{Al}(\text{Cu}, \text{Fe})$  solid solution is a stable phase.



**FIGURE 1.** The XRD patterns of the as-milled  $\text{Al}_{70}\text{Cu}_{20}\text{Fe}_{10}$  powders with milling times.



**FIGURE 2.** The XRD patterns of the as-milled  $\text{Al}_{70}\text{Cu}_{20}\text{Fe}_{10}$  alloys annealed at  $700^\circ\text{C}$  for 4 h.

The radial distribution functions (RDF) obtained from the Fourier transformation of the Fe and Cu K-edge  $k^3\chi(k)$  spectra are displayed in Figure 3(a) and (b) for the as-milled  $\text{Al}_{70}\text{Cu}_{20}\text{Fe}_{10}$  samples. In Figure 3(a), it can be observed that the Fe K-edge RDF profiles of the as-milled samples are basically the same except the slight decrease in amplitude with the milling time. This indicates that the coordination environment of bcc  $\alpha$ -Fe structure is almost unchanged during the milling process. On the contrary, the change of coordination environment of Cu atoms is obviously dependent on the milling time. For the sample milled for 5 h, the local structure around Cu atoms remains the fcc structure. However, the RDF shape of the 10h-milled  $\text{Al}_{70}\text{Cu}_{20}\text{Fe}_{10}$  becomes significantly different from that of the  $\text{Al}_{70}\text{Cu}_{20}\text{Fe}_{10}$  (5h), and the amplitude of the first peak decreases rapidly to about 25% of the latter. The strong decrease of magnitude is attributed to two factors. One is the large disorder in the Cu-containing alloy phase, and the other is the weak back scattering atom of Al in the first neighbor around Cu atoms in the  $\text{Al}_2\text{Cu}$  compound. With the milling time rising to 20 and 40 h, the intensity of the RDF peak of Cu atoms in the as-milled  $\text{Al}_{70}\text{Cu}_{20}\text{Fe}_{10}$  increases greatly.

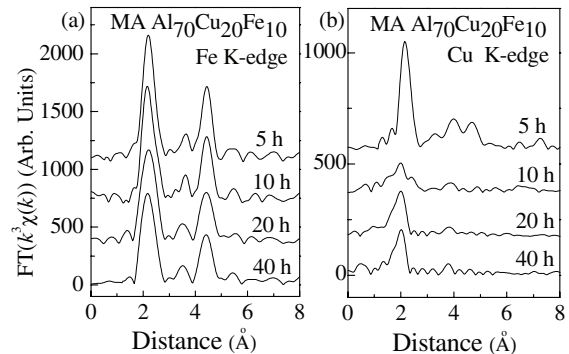


**FIGURE 3.** The radial distribution functions by Fourier transforming the  $k^3\chi(k)$  spectra of the Fe K-edge (a) and the Cu K-edge (b) of the as-milled  $\text{Al}_{70}\text{Cu}_{20}\text{Fe}_{10}$  alloys.

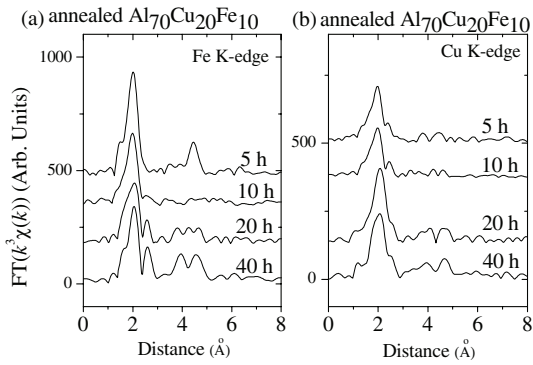


**FIGURE 4.** The radial distribution functions by Fourier transforming the Fe K-edge (a) and Cu K-edge (b)  $k^3\chi(k)$  spectra of the MA  $\text{Al}_{70}\text{Cu}_{20}\text{Fe}_{10}$  alloys annealed at 700°C for 4 h.

Figures 4(a) and (b) shows the RDF of Fe and Cu atoms for the annealed  $\text{Al}_{70}\text{Cu}_{20}\text{Fe}_{10}$  samples. From Figure 4(a), we can see that the annealing treatment strongly influences the local structure around Fe atoms. For the annealed  $\text{Al}_{70}\text{Cu}_{20}\text{Fe}_{10}$  (10h), the high shell peaks dramatically decrease. This suggests that the disorder around Fe atoms in the icosahedral QC phase is large. However, for the annealed  $\text{Al}_{70}\text{Cu}_{20}\text{Fe}_{10}$  (40h), the amplitude intensity of high shell peaks increases, and the RDF shape of Fe atoms is slightly similar to that of Cu K-edge XAFS result. It indicates that all the Fe atoms have incorporated into the AlCu alloy to form a single phase of  $\text{Al}(\text{Cu}, \text{Fe})$  solid solution. Figure 4 show that the RDF curves of Fe and Cu K-edge EXAFS spectra of the annealed  $\text{Al}_{70}\text{Cu}_{20}\text{Fe}_{10}$  (10h) are almost the same as those of the  $\text{Al}_{70}\text{Cu}_{20}\text{Fe}_{10}$  (5h). It means that the local structures of Fe and Cu atoms in the icosahedral QC phase are identical to those of Fe and Cu atoms in the  $\text{Al}_7\text{Cu}_2\text{Fe}$  compound.

We have fitted the main peak from 1.5 to 3.0 Å in the Fourier transformed  $R$ -space of Fe and Cu K-edge EXAFS by including the first and second nearest neighbors for the as-milled and annealed  $\text{Al}_{70}\text{Cu}_{20}\text{Fe}_{10}$  samples. The non-Gaussian distribution function was used where the structural disorder  $\sigma_s$  was modeled by a weighted exponential distribution function [9]. The theoretical back-scattering amplitude  $f(k)$  and phase shift  $\delta(k)$  functions were calculated by FEFF7 code [10]. The obtained structural parameters are summarized in Table 1.

**TABLE 1.** The structural parameters of the MA  $\text{Al}_{70}\text{Cu}_{20}\text{Fe}_{10}$  (10h) and the MA  $\text{Al}_{70}\text{Cu}_{20}\text{Fe}_{10}$  (40h) obtained from the XAFS fitting.

Sample	Shell	N	R(Å)	$\sigma_s^2$ (Å <sup>2</sup> )	$\sigma_t^2$ (Å <sup>2</sup> )
MA-10h	Fe-Fe	8	2.48(4)	0.0010(16)	0.0056(15)
	Fe-Fe	6	2.83(5)	0.0016(25)	0.0073(20)
	Cu-Cu	2	2.43(3)	0.0256(16)	0.0079(22)
	Cu-Al	8	2.58(3)	0.0289(25)	0.0075(31)
MA-40h	Fe-Fe	8	2.48(3)	0.0030(10)	0.0056 (20)
	Fe-Fe	6	2.82(6)	0.0049(36)	0.0073(16)
	Cu-Al	8	2.53(1)	0.0206(14)	0.0057(16)
	Cu-Cu	6	2.94(3)	0.0036(19)	0.0099(34)
Annealed-10h	Fe-Al	9	2.49(3)	0.0150(10)	0.0061(15)
	Cu-Al	8	2.55(1)	0.0161(18)	0.0056(19)
	Cu-Cu	2	2.61(3)	0.0164(15)	0.0097(20)
Annealed-40h	Fe-Al	8	2.51(3)	0.0099(16)	0.0057(18)
	Fe-Fe	6	2.94(4)	0.0124(40)	0.0099(31)
	Cu-Al	8	2.56(1)	0.0101(16)	0.0058(18)
	Cu-Cu	6	2.94(9)	0.0129(19)	0.0096(19)

With the milling time (see Table 1) increasing from 5 to 40 h, the local structure of Fe atoms in the as-milled  $\text{Al}_{70}\text{Cu}_{20}\text{Fe}_{10}$  keeps the structure of bcc  $\alpha$ -Fe. However, the structural disorder  $\sigma_s^2$  for the Fe-Fe pair increases slightly with the milling times, from 0.001 to 0.003 Å<sup>2</sup>. For the structural parameters of Cu atoms in the as-milled  $\text{Al}_{70}\text{Cu}_{20}\text{Fe}_{10}$  (10h), we have found that the bond length  $R$  for the Cu-Cu pair is different from that of fcc Cu, and the structural disorder of  $\sigma_s^2$  (about 0.03 Å<sup>2</sup>) for the Cu-Cu and Cu-Al pairs is much larger than that (0.001 Å<sup>2</sup>) of the Fe-Fe pair. This indicates that the local structural evolution around Cu atoms is different from that of Fe atoms with the milling time. Hence, the MA could not drive Fe to form CuFe or  $\text{Al}(\text{Cu}, \text{Fe})$  alloy with Cu and Al powders together. This result is different from those previous results of the MA CuFe alloys that showed that Cu and Fe can easily form a metastable alloy solid solution by mechanical alloying [11]. This illustrates that Al atoms in the AlCu alloy prevent Fe from entering the lattice of AlCu alloy. Seen from Table 1, the structural parameters of Cu atoms in the  $\text{Al}_{70}\text{Cu}_{20}\text{Fe}_{10}$  samples milled for 10 and 40 h, are similar to the references  $\text{Al}_2\text{Cu}$  compound and AlCu solid solution, respectively [8]. Therefore, at the initial stage of MA, part of Cu powder has been incorporated into the lattice of fcc Al to form the  $\text{Al}_2\text{Cu}$  compound. Finally, a homogenous AlCu solid solution is formed at the elongated milling of 40 h.

The XRD results have confirmed that the  $\text{Al}_7\text{Cu}_2\text{Fe}$  compound, the icosahedral  $\text{Al}_{65}\text{Cu}_{20}\text{Fe}_{15}$  QC alloy and the  $\text{Al}(\text{Cu}, \text{Fe})$  solid solution are the main resultant products for the annealed  $\text{Al}_{70}\text{Cu}_{20}\text{Fe}_{10}$  (5h),  $\text{Al}_{70}\text{Cu}_{20}\text{Fe}_{10}$  (10h) and  $\text{Al}_{70}\text{Cu}_{20}\text{Fe}_{10}$  (40h), respectively. From Table 1 we can see that the Fe-Al and Fe-Fe pairs in the icosahedral  $\text{Al}_{65}\text{Cu}_{20}\text{Fe}_{15}$  QC phase have nearly the same bond lengths as those in

$\text{Al}_7\text{Cu}_2\text{Fe}$  compound, while their structural disorder degrees are slightly larger. For the icosahedral QC phase there are only 9 Al atoms around a Fe atom with the distance of 2.50 Å [12]. For the  $\text{Al}(\text{Cu}, \text{Fe})$  solid solution, the first and second neighbors are 8 Al atoms and 6 Cu (or Fe) atoms with the bond lengths of 2.55 and 2.95 Å for Fe-Al and Fe-Cu (or Fe) pairs, respectively. These results show that the local environment around Fe atoms in the icosahedral QC is slightly similar to that of Fe atoms in  $\text{Al}_7\text{Cu}_2\text{Fe}$  compound, while much different from that of  $\text{Al}(\text{Cu}, \text{Fe})$  solid solution. This is also the case for Cu atoms in the icosahedral QC phase. Furthermore, The structural disorders around Fe and Cu atoms in the icosahedral QC phase are about 50% larger than those of the  $\text{Al}(\text{Cu}, \text{Fe})$  solid solution.

## CONCLUSIONS

XRD and XAFS are used to study the structural evolution of the mechanically alloyed ternary  $\text{Al}_{70}\text{Cu}_{20}\text{Fe}_{10}$  powders with milling time and annealing treatment. It is evident that, in the initial stage, mechanical alloying can drive the  $\text{Al}_{70}\text{Cu}_{20}\text{Fe}_{10}$  mixture to form an  $\text{Al}_2\text{Cu}$  compound but not an  $\text{AlFe}$  alloy,. With the milling time going to 20 h, an  $\text{AlCu}$  solid solution can be formed. Hence, the fcc structural Cu is easy to incorporate into the fcc structural Al to form  $\text{Al}_2\text{Cu}$  alloy using the MA method, while the bcc structural  $\alpha$ -Fe and fcc structural Al are difficult to be alloyed into  $\text{AlFe}$  alloy. The annealing at 700 °C for 4 h can drive the Fe atoms in the bcc structural  $\alpha$ -Fe to enter the lattice of the fcc structural Al and the fcc structural  $\text{AlCu}$  alloy phases. The main product of annealing can be  $\text{Al}_7\text{Cu}_2\text{Fe}$  compound, icosahedral QC alloy

and fcc  $\text{Al}(\text{Cu}, \text{Fe})$  alloy solid solution, depending on the milling time for the  $\text{Al}_{70}\text{Cu}_{20}\text{Fe}_{10}$  mixture.

## ACKNOWLEDGEMENTS

This project was supported by the National Natural Science Foundation of China (Grant No. 20303014) and the Cooperation Program between BSRF and NSRL.

## References

1. B.L. French, M.J. Daniels, J.C. Bilello, *J. Phys. D: Appl. Phys.* **38**, A44 (2005).
2. P. Barua, B.S. Murty, V. Srinivas, *Mater. Sci. Eng. A* **304-306**, 863 (2001).
3. B.S. Murty, R.V. Koteswara Rao, N.K. Mukhopadhyay, *J. Non Cryst. Solids* **334-335**, 48 (2004).
4. V. Srinivas, P. Barua, T.B. Ghosh, B.S. Murty, *J. Non Cryst. Solids* **334-335**, 540 (2004).
5. P. Barua, B.S. Murty, B.K. Mathur, V. Srinivas, *J. Appl. Phys.* **91**, 5353 (2002).
6. S.Q. Wei, H. Oyanagi, Z.R. Li, X.Y. Zhang, W.H. Liu, S.L. Yin, X.G. Wang, *Phys. Rev. B* **63**, 224201 (2001).
7. W.J. Zhong, S.Q. Wei, *J. Univ. Sci Tech.* **31**, 328 (2001).
8. 1999 JCPDS, International Centre for Diffraction Data.
9. X-ray Absorption: Principles, Applications, Techniques of EXAFS, SESAFS, and XANES, edited by D. C. Koningsberger and R. Prins (John wily, New York, 1988), p385.
10. J.J. Rehr, S.I. Zabinsky, R.C. Albers, *Phys. Rev. Lett.* **38**, 3397 (1992).
11. P.J. Schilling, J.-H. He, J. Cheng, E. Ma, *Appl. Phys. Lett.* **68**, 767 (1996).
12. G.T. Laissardiere, Z. Dankhazi, E. Belin, A. Sadoc, N.M. Duc, D. Mayou, M.A. Keegan and D.A. Papaconstantopoulos, *Phys. Rev. B* **51**, 14035 (1995)